PHYSICAL REVIEW B **83**, 161202(R) (2011)

# Control of the band-gap states of metal oxides by the application of epitaxial strain: The case of indium oxide

Aron Walsh* and C. Richard A. Catlow
*University College London, Department of Chemistry, Materials Chemistry, Third Floor, Kathleen Lonsdale Building, Gower Street, London WC1E 6BT, United Kingdom*

K. H. L. Zhang and Russell G. Egdell
*Department of Chemistry, Chemistry Research Laboratory, University of Oxford, Mansfield Road, Oxford OX1 3TA, United Kingdom*
(Received 14 March 2011; published 12 April 2011)

We demonstrate that metal oxides exhibit the same relationship between lattice strain and electronic band gap as nonpolar semiconductors. Epitaxial growth of ultrathin [111]-oriented single-crystal indium-oxide films on a mismatched Y-stabilized zirconia substrate reveals a net band-gap decrease, which is dissipated as the film thickness is increased and the epitaxial strain is relieved. Calculation of the band-gap deformation of $In_2O_3$, using a hybrid density functional, confirms that, while the uniaxial lattice contraction along [111] results in a band-gap *increase* due to a raise of the conduction band, the lattice expansion in the (111) plane caused by the substrate mismatch compensates, resulting in a net band-gap *decrease*. These results have direct implications for tuning the band gaps and transport properties of oxides for application in optoelectronic devices.

DOI: 10.1103/PhysRevB.83.161202 PACS number(s): 78.66.Nk, 61.72.jn, 65.40.De, 71.20.−b

The control of electronic states in nonpolar semiconductors through dilation of the crystal lattice was first explored in detail by Bardeen and Shockley.[1] In general, as a lattice contracts, the splitting between the bonding valence states and antibonding conduction states increases, resulting in a net band-gap increase; the effect is quantified through the characteristic band-gap deformation potential

$$\alpha_V = \frac{\partial E_g}{\partial \ln V}, \tag{1}$$

where V represents the unit-cell volume. Typically, for covalent semiconductors, $\alpha_v$ is a large negative number, e.g., −24 eV for C and −11 eV for Si at the Γ point.[2] The sensitive dependence of the electronic band structure on elastic strain can be used to tune the band gap and, hence, light absorption, emission, and transport properties.[3–5]

Conductive metal oxides are now widely used for optoelectronic applications,[6] where their transparency and interfacial electron transfer properties are highly sensitive to the material band gap. For example, in organic solar cells, the conduction-band level of Sn-doped $In_2O_3$ (ITO) must be as low as possible to maximize the open-circuit voltage,[7] while in photoelectrochemical water splitting, the conduction-band level of the photoanode (e.g., $TiO_2$) must be high enough to make the chemical reduction of $H^+$ to $H_2$ thermodynamically favorable.[8]

In this Rapid Communication, we demonstrate that the electronic states of heteropolar metal oxides can be tuned in the same way as traditional semiconductor materials. The growth of ultrathin single-crystal thin films of $In_2O_3$ on a strained Y-stabilized $ZrO_2$ substrate reveals a redshift in the onset of optical absorption, which is alleviated as the film thickness increases and the bulk lattice constant is approached. These observations are confirmed through hybrid density functional calculations, which highlight that oxides can exhibit similar band-gap deformation effects as traditional III–V and II–VI semiconductor materials, and that the compensating uniaxial strain is not enough to offset the band-gap changes arising from the tensile epitaxial strain. Furthermore, we demonstrate that both band-gap contraction and expansion can in principle be achieved through appropriate choice of growth substrate. These effects remain to be exploited in a range of oxide applications.

Indium sesquioxide is a widely used transparent conducting metal oxide,[9] and its defect properties have been the subject of intense research.[10–16] One major difficulty has been in the growth of high-quality $In_2O_3$ samples; however, we have recently succeeded in synthesizing $In_2O_3$ and ITO single-crystal thin films on Y-stabilized cubic zirconia (YSZ) by oxygen-plasma assisted molecular beam epitaxy.[17] The bixbyite structure of $In_2O_3$ is in fact a defective $2 \times 2 \times 2$ supercell of the face-centered-cubic fluorite structure of YSZ. The lattice parameter $2a = 10.292$ Å for 17% Y concentration in YSZ compares favorably to 10.117 Å for the bulk $In_2O_3$ lattice, but a mismatch of 1.7% is present.

All films were grown on a heated substrate (700 °C) in ultrahigh vacuum; an atomically sharp interface between $In_2O_3$ and YSZ was confirmed through high-resolution transmission electron microscopy measurements. The lattice strain in the [111]-oriented $In_2O_3$ epilayer was measured with the film thickness from 35 to 420 nm by mapping the (222) reflection observed in the $\theta$-$2\theta$ x-ray diffraction pattern. The out-of-plane lattice spacing in the [111] direction ($\frac{a}{\sqrt{3}}$) varies from 5.764 to 5.821 Å, exhibiting compressive strain from the bulk value of 5.841 Å, as shown in Fig. 1. The in-plane lattice spacing ($\sqrt{2}a$), determined using Poisson's ratio ($\gamma$), exhibits a tensile strain from 14.489 to 14.360 Å above the equilibrium bulk value of 14.306 Å.

The measured optical absorption data for the 35- and 420-nm thin films of $In_2O_3$ are shown in Fig. 1. There is a distinct redshift in the onset of optical absorption to longer wavelengths as the film thickness decreases from 3.56 eV (420 nm) to 3.48 eV (35 nm). It was not possible to obtain useful absorption data for films of intermediate thickness owing

 

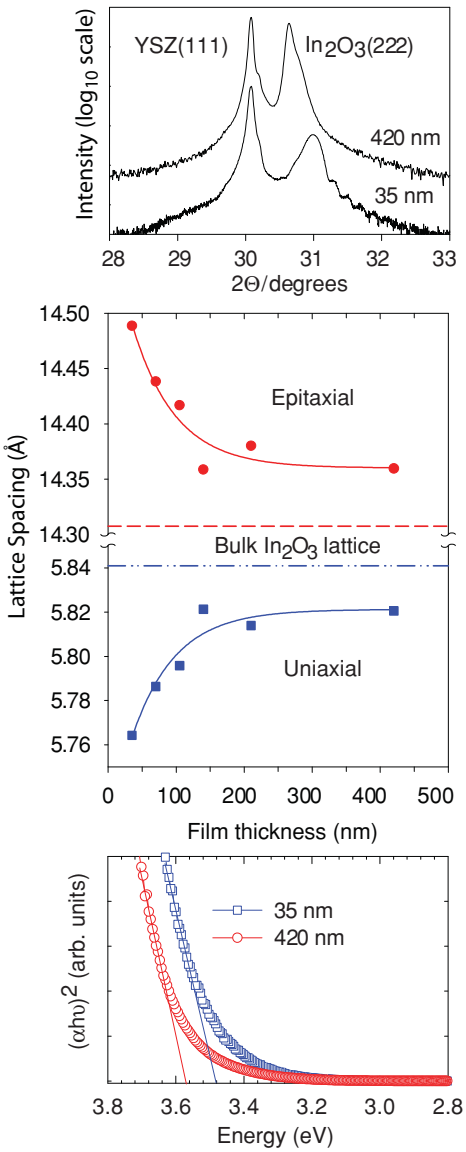


FIG. 1. (Color online) The top panel shows $\theta$-$2\theta$ x-ray diffraction profiles for 35- and 420- nm thin films of $In_2O_3$ presented on a logarithmic scale. The center panel shows the measured in-plane ($a\sqrt{2}$) and out-of-plane ($a/\sqrt{3}$) lattice constants as a function of $In_2O_3$ film thickness. The dashed lines show the values expected for a fully relaxed bulklike single-crystal film of $In_2O_3$. The lower panel shows the measured optical absorption spectra for the 35- and 420-nm films, with intercepts at 3.48 and 3.56 eV, respectively.

to the appearance of deep pinholes and trenches associated with a wetting-dewetting transition.[18] These imperfections cause significant light scattering for films thicker than about 50 nm, and the films assume a milky appearance before they eventually fill in for thicknesses greater than 200 nm.

It was recently demonstrated that the fundamental band gap of $In_2O_3$ is dipole forbidden, with strong optical transitions originating from 0.8 eV below the top of the valence band,[19] which is consistent with calculations at the level of many-body perturbation theory.[20] The measurements reported here refer to the direct optical band gap, which includes Moss-Burstein[21] effects, as well as optical selection rules. X-ray photoemission spectra have been measured to track the valence-band-edge shift; however, the movement is complicated by thickness-dependent band bending.[22]

Evaluation of the hydrostatic bulk deformation potential of $In_2O_3$ [Eq. (1)] was performed using a hybrid density functional (HSE06),[23] as implemented in the Vienna *ab initio* simulation package (VASP),[24] which has demonstrated recent successes in describing the electronic properties of dielectric materials.[25–28] A $3 \times 3 \times 3$ $k$-point mesh was used for the bulk lattice, with a well-converged 500-eV plane-wave cutoff. The semicore In $4d$ states were treated explicitly as valence, including scalar-relativistic effects. The equilibrium lattice constant ($a_{\mathrm{HSE}} = 10.156$ Å) is in very good agreement with experiment.

Remarkably, we have calculated $\alpha_v = -4.21$ eV in the bulk material, which is comparable to the value for GaN and other III–V and II–VI semiconductors.[2,29–32] Hydrostatic lattice strain of 2.5% would result in a band-gap change of 0.1 eV. The band-gap deformation contains contributions from the movement of both empty and occupied band-edge states, i.e., $\alpha_V = \alpha_{\mathrm{CBM}} - \alpha_{\mathrm{VBM}}$. To assign these contributions, we have further calculated the valence-band-maximum (VBM) and conduction-band-minimum (CBM) absolute deformation potentials to be $\alpha_{\mathrm{VBM}} = -0.10$ eV and $\alpha_{\mathrm{CBM}} = -4.31$ eV.[33] These values are determined by an intricate combination of the electrostatic potential, orbital interaction, and kinetic energy changes, but the clear result is that the shift in the conduction band (a delocalized In $5s$ derived state) is the dominant driving force for the observed band-gap alterations.

To explore the band-gap−substrate relationship in more detail, we have explicitly considered a [111]-oriented hexagonal supercell of the bixbyite structure, using a lattice vector transformation matrix of the form

$$\begin{pmatrix} -1 & 0 & 1 \\ 0 & 1 & -1 \\ 1 & 1 & 1 \end{pmatrix}.$$

Calculations were then performed as a function of the epitaxial lattice spacing. The relaxed uniaxial lattice spacing was found to exhibit the Poisson effect, i.e., under epitaxial conditions, the perpendicular response to the two-dimensional epitaxial strain is restricted to a single line defined by Poisson's ratio[34]

$$\epsilon_{\perp} = \frac{-2\gamma\epsilon_{||}}{1-\gamma}. \qquad (2)$$

It should be noted that, for the synthesized films of $In_2O_3$, the epitaxial strain ($\epsilon_{||}$) is positive due to the larger substrate lattice spacing, and the compensating uniaxial strain ($\epsilon_{\perp}$) is negative. Computational modeling of $In_2O_3$ using a carefully parameterized interatomic potential resulted in a value of $\gamma = 0.323$,[35] which is typical for metal oxides; the upper limit for an elastically isotropic material is $\gamma = 0.5$.[36]

The predicted band-gap changes are plotted in Fig. 2 for a range of epitaxial lattice spacings, explicitly taking into account the effect of the compensating uniaxial strain. For each case, the trends in the optical and electronic band gaps are equivalent, i.e., even under conditions of epitaxial strain where the lattice symmetry is reduced from body-centered-cubic ($Ia\bar{3}$) to trigonal ($R\bar{3}$), the lowest energy band to band optical transitions[37,38] remain dipole forbidden for both parallel and

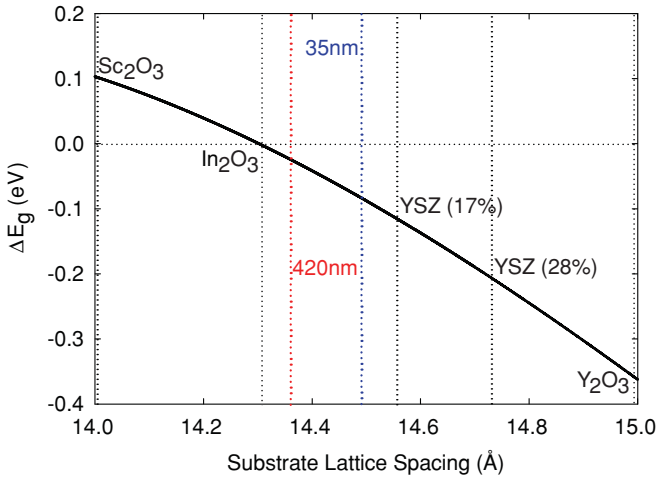


FIG. 2. (Color online) Predicted band-gap changes arising from epitaxial strain for a [111]-oriented $In_2O_3$ single crystal, inclusive of the compensating uniaxial strain. The lattice constants for a range of substrate materials are shown with vertical dotted lines. The predictions compare well to two measured points for 35- and 420-nm thin films of $In_2O_3$ grown on YSZ, where $\Delta E_g = 0.08$ eV (see Fig. 1).

perpendicular polarization of the incident light. Therefore, the onset of strong optical transitions still originates from below the top of the valence band. The predicted band-gap changes are within 10 meV of those expected from an isotropic volume change, i.e., $\Delta E_g \simeq \alpha_v \frac{\Delta V}{V}$. For highly mismatched $In_2O_3$ films, the calculated band-gap variation extends to 0.5 eV over the 1 Å substrate range as shown in Fig. 2.

The accessible range for coherent epitaxial strain is substantial when one considers the variety of commercially available substrates that are compatible with the bixbyite structure, e.g., compressive: $Sc_2O_3$ ($2a = 9.9$ Å) and tensile: 28% Y-stabilized $ZrO_2$ ($2a = 10.4$ Å), which result in $-2\%$ and 3% epitaxial mismatch, respectively. The band-gap range can be further extended by limiting the extent of compensating strain through the formation of confined structures (superlattices or core-shell structures) or through the application of external pressure.

It has recently been demonstrated that compressive straining of $TiO_2$ thin films results in increased visible light absorption,[39,40] which can be explained in the same way as $In_2O_3$. In effect, tensile strain is equivalent to a negative pressure that weakens the electrostatic potential, as well as the bonding interactions, which serves to narrow the band gap predominately through a lowering of the conduction band (an increase of the electron affinity). These are general effects, which can be exploited in a wider range of metal-oxide systems, either through a judicious choice of growth substrate or through the use of material interfaces and superlattices that introduce coherent lattice strain. In contrast to traditional semiconducting materials, metal oxides are more suitable for high-temperature applications and, hence, the differences in material thermal expansion coefficients can also be exploited in a similar fashion.

In conclusion, we have demonstrated the control of the band gap of indium oxide through epitaxial growth on a mismatched substrate. By comparing with first-principles electronic structure calculations, we find that this should be a general effect in metal oxides and can be used to tune the band-edge positions as a function of epitaxial strain. The implications of this phenomenon are broad ranging, in particular, strain may be used to control the redox potentials associated with oxide-based electrochemical devices in addition to open-circuit voltages in photovoltaic systems.

A.W. and C.R.A.C. would like to acknowledge support from EPSRC Grant No. EP/F067496. K.H.L.Z. would like to thank the Oxford Clarendon Fund for financial support. The Oxford MBE project was initially supported by EPSRC Grant No. GR/S94148.

*a.walsh@ucl.ac.uk

[1] J. Bardeen and W. Shockley, Phys. Rev. **80**, 72 (1950).
[2] S.-H. Wei and A. Zunger, Phys. Rev. B **60**, 5404 (1999).
[3] G. H. Olsen, C. J. Nuese, and R. T. Smith, J. Appl. Phys. **49**, 5523 (1978).
[4] E. D. Minot, Y. Yaish, V. Sazonova, J.-Y. Park, M. Brink, and P. L. McEuen, Phys. Rev. Lett. **90**, 156401 (2003).
[5] D. C. Houghton, G. C. Aers, N. L. Rowell, K. Brunner, W. Winter, and K. Eberl, Phys. Rev. Lett. **78**, 2441 (1997).
[6] P. P. Edwards, A. Porch, M. O. Jones, D. V. Morgan, and R. M. Perks, Dalton Trans. **15**, 2295 (2004).
[7] N. R. Armstrong, P. A. Veneman, E. Ratcliff, D. Placencia, and M. Brumbach, Acc. Chem. Res. **42**, 1748 (2009).
[8] Y. Gai, J. Li, S.-S. Li, J.-B. Xia, and S.-H. Wei, Phys. Rev. Lett. **102**, 036402 (2009).
[9] I. Hamberg, C. G. Granqvist, K. F. Berggren, B. E. Sernelius, and L. Engstrom, Phys. Rev. B **30**, 3240 (1984).
[10] Y. Ohya, T. Yamamoto, and T. Ban, J. Am. Ceram. Soc. **91**, 240 (2008).
[11] J. H. W. DeWit, J. Solid State Chem. **20**, 143 (1977).
[12] R. L. Weiher, J. Appl. Phys. **33**, 2834 (1962).
[13] S. Lany and A. Zunger, Phys. Rev. Lett. **98**, 045501 (2007).
[14] T. Tomita, K. Yamashita, Y. Hayafuji, and H. Adachi, Appl. Phys. Lett. **87**, 051911 (2005).
[15] P. Ágoston, K. Albe, R. M. Nieminen, and M. J. Puska, Phys. Rev. Lett. **103**, 245501 (2009).
[16] A. Walsh, J. L. F. Da Silva, and S.-H. Wei, Phys. Rev. B **78**, 075211 (2008).
[17] A. Bourlange, D. J. Payne, R. G. Egdell, J. S. Foord, P. P. Edwards, M. O. Jones, A. Schertel, P. J. Dobson, and J. L. Hutchison, Appl. Phys. Lett. **92**, 092117 (2008); K. H. L. Zhang, A. Walsh, C. R. A. Catlow, V. K. Lazarov, and R. G. Egdell, Nano Letters **10**, 3740 (2010).
[18] M. Coll, J. Gázquez, A. Pomar, T. Puig, F. Sandiumenge, and X. Obradors, Phys. Rev. B **73**, 075420 (2006).
[19] A. Walsh, J. L. F. Da Silva, S.-H. Wei, C. Körber, A. Klein, L. F. J. Piper, A. DeMasi, K. E. Smith, G. Panaccione, P. Torelli,

D. J. Payne, A. Bourlange, and R. G. Egdell, Phys. Rev. Lett. **100**, 167402 (2008).

[20]F. Fuchs and F. Bechstedt, Phys. Rev. B **77**, 155107 (2008).

[21]T. S. Moss, Proc. Phys. Soc., London, Sect. B **67**, 775 (1954).

[22]P. D. C. King, T. D. Veal, D. J. Payne, A. Bourlange, R. G. Egdell, and C. F. McConville, Phys. Rev. Lett. **101**, 116808 (2008).

[23]A. V. Krukau, O. A. Vydrov, A. F. Izmaylov, and G. E. Scuseria, J. Chem. Phys. **125**, 224106 (2006).

[24]G. Kresse and J. Furthmüller, Phys. Rev. B **54**, 11169 (1996).

[25]J. Paier, M. Marsman, K. Hummer, G. Kresse, I. C. Gerber, and J. G. Angyan, J. Chem. Phys. **124**, 154709 (2006).

[26]J. Paier, M. Marsman, and G. Kresse, Phys. Rev. B **78**, 121201 (2008).

[27]S. J. Clark, J. Robertson, S. Lany, and A. Zunger, Phys. Rev. B **81**, 115311 (2010).

[28]J. Vidal, F. Trani, F. Bruneval, M. A. L. Marques, and S. Botti, Phys. Rev. Lett. **104**, 136401 (2010).

[29]A. Janotti and C. G. Van de Walle, Phys. Rev. B **75**, 121201 (2007).

[30]Y. Z. Zhu, G. D. Chen, H. Ye, A. Walsh, C. Y. Moon, and S.-H. Wei, Phys. Rev. B **77**, 245209 (2008).

[31]Y. H. Li, X. G. Gong, and S.-H. Wei, Appl. Phys. Lett. **88**, 042104 (2006).

[32]C. G. Van de Walle, Phys. Rev. B **39**, 1871 (1989).

[33]Calculation of the absolute deformation potential relies on an absolute energy reference to which the Kohn-Sham eigenvalues can be aligned: We have chosen the vacuum level from the nonpolar (111) surface of $In_2O_3$ (240-atom-layer slab with 20 Å vacuum spacing within periodic boundary conditions). For details of the structural model see A. Walsh and C. R. A. Catlow, J. Mater. Chem. **20**, 10438 (2010).

[34]A. Segmüller, J. Vac. Sci. Technol. A **9**, 2477 (1991).

[35]A. Walsh, C. R. A. Catlow, A. A. Sokol, and S. M. Woodley, Chem. Mater. **21**, 4962 (2009).

[36]G. Grimvall, *Thermophysical Properties of Materials* (Elsevier, Amsterdam, 1999).

[37]The optical transition matrix elements were calculated from the Kohn-Sham eigenvalues using Fermi's Golden Rule. Transitions to the lowest-lying conduction band were all of intensity of less than 0.05 a.u. from the top of the valence band, while from 0.8 eV below, the transition intensity increases to more than 0.8 a.u.

[38]B. Adolph, J. Furthmüller, and F. Bechstedt, Phys. Rev. B **63**, 125108 (2001).

[39]T. Shibata, H. Irie, and K. Hashimoto, J. Phys. Chem. B **107**, 10696 (2003).

[40]W.-J. Yin, S. Chen, J.-H. Yang, X. Gong, Y. Yan, and S.-H. Wei, Appl. Phys. Lett. **96**, 221901 (2010).